

THE CHEMICAL COMPOSITION OF BLUE HORIZONTAL BRANCH STARS IN M4 AND NGC 6397

DAVID L. LAMBERT,¹ ANDREW MCWILLIAM,² AND VERNE V. SMITH^{1,3}

Received 1991 July 10; accepted 1991 August 21

ABSTRACT

High-resolution ($\lambda/\Delta\lambda \simeq 18,000$) spectra of two horizontal branch stars in M4 and one in NGC 6397 provide a metallicity in good agreement with the values obtained previously by others from analyses of cluster red giants. For one HB star in M4, the C, N, O abundances derived from near-infrared C I, N I, and O I lines are consistent with those obtained for red giants by Brown et al. (1990). This result suggests that the He-core flash cannot always result in products of He-burning being mixed into the envelope.

Subject headings: globular clusters: individual (M4, NGC 6397) — stars: abundances — stars: giant — stars: horizontal-branch

1. INTRODUCTION

Horizontal branch stars are helium core burning stars of low metallicity. The blue horizontal-branch (BHB) stars are most probably stars with an envelope of lower than average mass around a core of mass quite similar to that of other HB stars, i.e., the RR Lyrae variables and the red HB stars. The BHB and other HB stars have evolved from giants on the red giant branch (RGB) via the He-core flash at the tip of the RGB. On exhaustion of He in the core, a BHB star is expected to evolve to the asymptotic giant branch (AGB). This sketch of the evolution shows that the chemical compositions of the HB stars offer potential insights into nucleosynthesis and mixing on the AGB and on the RGB including the He-core flash.

There is the obvious role of the HB, especially the BHB stars, as a provider of independent data on the mixing sensitive abundances of C, N, and O. All of the now extensive data on mixing of CN-cycled material into the atmosphere of a RGB star are provided by analyses of molecular lines (CH, CN, CO) in spectra of RGB stars. The [O I] lines at 6300 and 6363 Å may monitor the presence of ON-cycled material. At the temperatures of BHB stars, C, N, as well as O abundances are obtainable from atomic (C I, N I, O I) lines. If it were shown that the “molecular” and “atomic” abundances gave consistent results, our confidence in both analyses would be enhanced. Of course, if the He-core flash induces the mixing of nuclear-processed material into the envelope, the compositions of the post-flash HB and pre-flash RGB stars will necessarily be different. Even in this event, the compositions of the HB and early-AGB giants should be similar and comparisons of “atomic” and “molecular” abundances provide a consistency check. If this check reveals an inconsistency, it should not, however, automatically be taken as indicating systematic errors in the HB and/or AGB analyses: the composition of the BHB star’s atmosphere may be modified by diffusion (Michaud, Vauclair, & Vauclair 1983), or additional mixing

may be initiated as a giant’s deep convective envelope redevelops on the transition from HB to AGB star. Finally, the HB stars, because they are hotter than the red giants, may offer opportunities to obtain certain elemental abundances unobtainable from the spectra of red giants; for example, in the hottest HB stars, He I lines may be detectable and so provide the informative He/H ratio; see, for example, the BHB stars in NGC 6752 for which the low He abundance (He/H \sim 0.03 at $T_{\text{eff}} \sim 16,000$ K) suggest gravitational settling of He (Heber et al. 1986).

Our study of HB stars in M4 and NGC 6397 was prompted by the analysis of Kodaira & Philip (1984, hereafter KP) of 2.5 Å mm⁻¹ image tube spectra of stars just to the blue of the RR Lyrae gap. KH claimed with some equivocation that the derived metallicities of [Fe/H] = -0.4 and -1.4 for M4 and NGC 6397, respectively, were the metallicities of the clusters. KP noted that spectroscopic analyses of cluster red giants led to lower values in both cases. Analyses of giants completed since 1984 have generally confirmed the values in the literature available to KP, and all of the analyses have arrived at cluster metallicities at least a factor of 3 (0.5 dex) below KP’s published values; for example, Zinn (1985) in his critical compilation gives [Fe/H] = -1.28 and -1.91 for M4 and NGC 6397, respectively.

If the cluster metallicity is that provided by the red giants, why are the BHB’s metal-rich relative to their RGB progenitors and their AGB descendants? To answer this question, we decided to acquire and analyze new high-resolution CCD spectra of KP’s stars. In the event that we confirmed the metallicity difference between the HB and RGB/AGB stars, we expected to have sufficient information on the elemental abundances to test several speculations as to the origins of the differences. In particular, we set out to determine the C, N, and O abundances, three elements not represented in KP’s spectra. If the higher metallicity of HB stars is due to diffusion, one would expect anomalous element-to-iron ratios. This expectation was not confirmed by KP who reported that the element-to-iron ratios for 10 elements from Al to Zr were normal (i.e., solar) to within the (large) errors of measurement. If extensive mixing and/or mass loss were provoked by the He-core flash, a BHB star’s atmosphere could be enriched in He and the strengths of the metal lines, which would be enhanced by the

¹ Department of Astronomy, University of Texas, Austin, TX 78712.

² Department of Astronomy, New Mexico State University, Las Cruces, NM 88003.

³ Visiting Astronomer, Cerro Tololo Inter-American Observatory, National Optical Astronomy Observatories, operated by the Association of Universities for Research in Astronomy, Inc., under contract with the National Science Foundation.

consequent reduction of the continuous opacity, would be interpreted as an *apparent* metal enrichment. Although He is not detectable in the rather cool HB stars in M4 and NGC 6397, such severe mixing might well result in anomalous ratios of C, N, and O.

2. OBSERVATIONS

We obtained spectra of the three HB stars observed by KP: two M4 stars, No. 4408 and No. 4632 (Lee 1977) and star No. 48 (Woolley et al. 1961) in NGC 6397. The spectra were acquired in 1988 July with the CTIO 4 m echelle spectrograph system and air schmidt camera, which gave a 2.5 pixel resolving power of about 18,000. We obtained blue spectra with complete wavelength coverage from 3820 to 4570 Å for all three stars, which required 6.5 hr for M4 No. 4408, 4 hr for NGC 6397 No. 48, and 3.5 hr for M4 No. 4632. These lengthy exposure times were due to the faintness of the stars, the low blue quantum efficiency of the GEC CCD, and low spectrograph efficiency at these short wavelengths. The total exposure times were split into 30 minute segments in order to reduce the number of cosmic ray strikes per echelle frame and allow for removal of cosmic rays from the final spectra. We estimate that the final S/N of our combined blue spectra was about 70–80, with the S/N improving towards the longer wavelengths.

We also obtained red spectra for M4 star No. 4408, which covered a continuous wavelength region from 8080 to 9620 Å, and included a number of C, N, and O lines. The exposure time required to provide a S/N of about 70–80 was only 2.5 hr despite significantly lower stellar flux, which was due to the high CCD quantum efficiency and high spectrograph efficiency in the red. A red spectrum of the hot star σ Sgr was taken, at a similar airmass, in order to identify and remove telluric features from the M4 No. 4408 spectrum; this was facilitated by division of the σ Sgr into the M4 No. 4408 spectrum.

Echelle orders from the individual frames were extracted using standard IRAF routines in the twod package, and were co-added using an algorithm which identified and removed the effects of cosmic ray strikes, based on the deviation from the median frame. The co-added cleaned, spectra were wavelength calibrated and equivalent widths then measured using standard IRAF routines. We chose not to co-add overlapping portions of consecutive orders, as this allowed us to obtain two independent measurements for most lines; weighted averages of the two equivalent width measurements were adopted and appear in Table 1. Identifications of lines were checked against the spectral atlas of field HB stars by Adelman, Fisher, & Hill (1987). Flattened examples of the spectra appear in Figures 1, 2, 3, and 4. KP adopt an alternative nomenclature for the M4 stars (see Greenstein 1939): M4 No. 4408 and No. 4632 are KP's M4–553 and M4–206, respectively.

With the exception of M4 No. 4408, the stellar lines are unresolved at our resolution. For M4 No. 4408, the line widths are greater than can be attributed to thermal plus microturbulent broadening. If the excess broadening is attributed entirely to the effect of stellar rotation, we obtain a projected rotational velocity $v \sin i \approx 14 \pm 4 \text{ km s}^{-1}$. In general, microturbulence is paired with macroturbulence of a comparable magnitude. If we assume that this pairing occurs for M4 No. 4408, we find $v \sin i \approx 12 \text{ km s}^{-1}$. For the other two stars, we find $v \sin i \lesssim 6 \text{ km s}^{-1}$ in the absence of macroturbulence. Our results for the two M4 stars are consistent with Peterson's (1985) observations of 9 HB star in M4 that indicated "the complete absence of rotation as large as $v \sin i = 15 \text{ km s}^{-1}$ ".

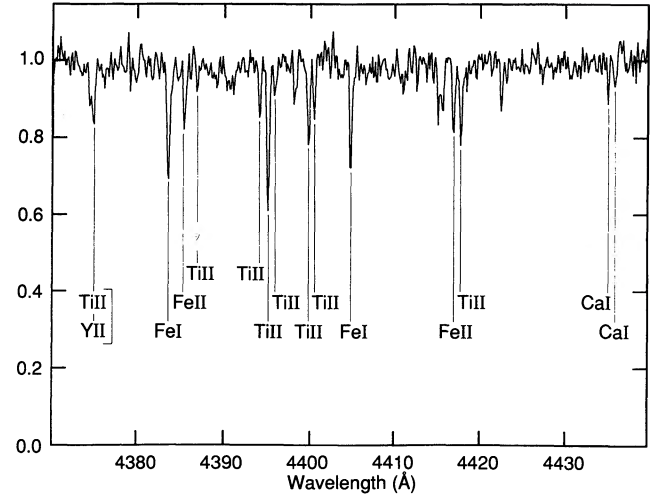


FIG. 1.—Spectrum of M4 No. 4408 from 4370 to 4440 Å.

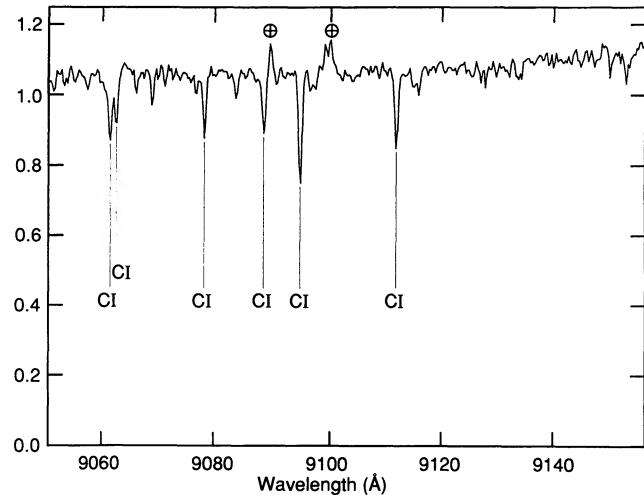


FIG. 2.—Red Spectrum of M4 No. 4408 showing C I lines near 9100 Å. Two apparent emission lines are due to imperfect cancellation of telluric lines.

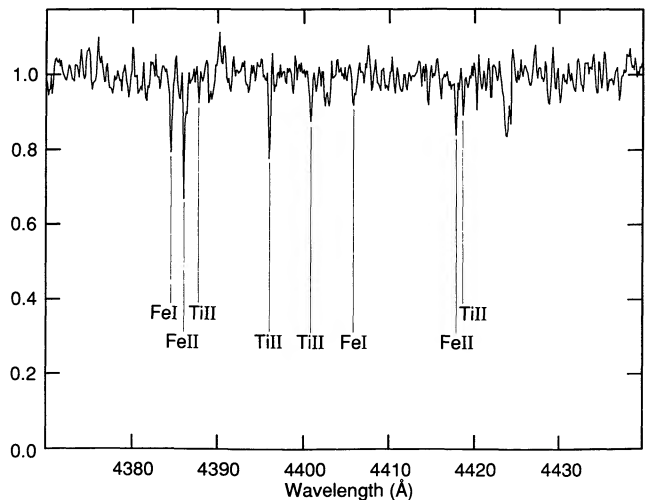


FIG. 3.—Spectrum of M4 No. 4632 from 4370 to 4440 Å.

TABLE 1
THE OBSERVED LINES AND DERIVED ABUNDANCES

SPECIES	λ (Å)	EP (eV)	$\log gf$	M4 No. 4408		M4 No. 4632		NGC 6397 No. 48	
				W_λ	$\log \epsilon$	W_λ	$\log \epsilon$	W_λ	$\log \epsilon$
Mg I	4057.515	4.34	-0.88	53	7.25
Mg I	4167.277	4.34	-0.73	63	7.20
Mg II	4481.210	8.86	0.97 ^a	111	5.33 ^a
Al I	3944.016	0.00	-0.64	125	5.67	67	5.34	44	5.15
Al I	3961.535	0.01	-0.34	88	5.00 ^b	61	4.99 ^b
Si I	3905.532	1.91	-1.09	89	6.36
Si II	3856.520	6.86	-0.65	43	5.82
Si II	3862.593	6.86	-0.90	124	7.08	26	5.75
Si II	4128.098	9.83	0.31	71	7.11	90	7.39
Si II	4130.856	9.84	0.48	54	6.72	85	7.08
Ca I	4226.740	0.00	0.24	136	5.47	60	4.98
Ca I	4283.014	1.89	-0.22	30	6.00	7:	5.58:
Ca I	4302.539	1.90	0.28	44	5.71	13:	5.37:
Ca I	4434.967	1.89	-0.01	28	5.74
Ca I	4435.688	1.89	-0.52	25	6.19
Sc II	4246.837	0.31	0.32	126	2.28	46	1.73	18	1.17
Sc II	4314.091	0.62	-0.10	85	2.50	52	2.42
Sc II	4324.998	0.60	-0.44	37	2.29
Sc II	4400.398	0.61	-0.28	44	2.22	16:	1.97:
Sc II	4415.563	0.60	-0.54	26	2.19
Ti II	3900.560	1.13	-0.45	37	3.20
Ti II	3913.470	1.12	-0.53	160	4.56	32	3.19
Ti II	4025.134	0.61	-1.98	72	4.61
Ti II	4028.346	1.89	-1.00	77	4.56	37	4.31
Ti II	4163.654	2.59	-0.40	80	4.45	59	4.43	10	3.42
Ti II	4171.908	2.60	-0.56	63	4.44	80	4.82
Ti II	4287.884	1.08	-2.02	51	4.72
Ti II	4290.226	1.16	-1.12	124	4.63	70	4.32
Ti II	4294.142	1.08	-1.11	109	4.41	43	3.95	18	3.42
Ti II	4300.053	1.18	-0.77	139	4.46	48	3.74	29	3.38
Ti II	4301.927	1.16	-1.16	70	4.12	34	3.92
Ti II	4307.880	1.16	-1.29	22	3.75
Ti II	4312.875	1.18	-1.16	95	4.39	54	4.20
Ti II	4314.981	1.16	-1.13	93	4.31	29	3.81
Ti II	4386.853	2.60	-1.26	20	4.49	26	4.82
Ti II	4394.068	1.22	-1.59	40	4.23
Ti II	4395.040	1.08	-0.66	135	4.56	78	3.88	28	3.18
Ti II	4395.848	1.24	-2.17	24	4.23
Ti II	4399.778	1.24	-1.27	71	4.28	55	4.36
Ti II	4417.723	1.16	-1.43	75	4.43	26	4.05
Ti II	4443.812	1.08	-0.70	120	4.09	81	3.95
Ti II	4444.562	1.12	-2.03	28	4.41
Ti II	4450.491	1.08	-1.45	57	4.21	23	3.95
Ti II	4464.457	1.16	-2.08	38	4.65	21	4.59
Ti II	4468.500	1.13	-0.60	118	4.00	97	4.03	24	3.07
Ti II	4488.329	3.12	-0.82	47	4.85	27	4.73
Ti II	4501.278	1.12	-0.75	124	4.20	86	4.07	19	3.10
Ti II	4529.490	1.57	-2.03	24	4.64	18:	4.73: ^b
Cr I	4274.806	0.00	-0.23	47	4.98
Cr II	4275.557	3.86	-1.45	17	4.68	8:	4.49:
Fe I	3820.436	0.86	0.15	133	6.13
Fe I	3825.891	0.91	0.00	158	6.69
Fe I	3849.977	1.01	-0.84	125	7.10
Fe I	3859.922	0.00	-0.68	142	6.48
Fe I	3865.533	1.01	-0.95	64	6.54
Fe I	3872.510	0.99	-0.89	108	6.92
Fe I	3878.027	0.95	-0.88	70	6.49
Fe I	3878.580	0.09	-0.88	149	6.86
Fe I	3899.719	0.09	-1.50	92	6.74	33	6.44
Fe I	3920.269	0.12	-1.71	77	6.82
Fe I	3922.923	0.05	-1.62	96	6.88
Fe I	3927.933	0.11	-1.51	86	6.70
Fe I	3930.308	0.09	-1.51	88	6.70
Fe I	4005.254	1.56	-0.58	62	6.50
Fe I	4045.825	1.48	0.31	142	6.47	60	5.82	22	5.32
Fe I	4063.605	1.56	0.09	104	6.26	62	6.11	23	5.61
Fe I	4071.749	1.61	0.01	89	6.23	38	5.92
Fe I	4132.067	1.61	-0.63	54	6.48	33	6.48
Fe I	4143.878	1.56	-0.43	59	6.30	46	6.43

TABLE 1—Continued

SPECIES	λ (Å)	EP (eV)	$\log gf$	M4 No. 4408		M4 No. 4632		NGC 6397 No. 48	
				W_λ	$\log \epsilon$	W_λ	$\log \epsilon$	W_λ	$\log \epsilon$
Fe I	4187.047	2.45	-0.51	40	6.75
Fe I	4187.812	2.42	-0.52	37	6.70
Fe I	4199.105	3.05	0.28	57	6.57	29	6.43
Fe I	4202.040	1.48	-0.67	59	6.49	20	6.18
Fe I	4227.440	3.33	0.28	55	6.73	24	5.54
Fe I	4235.949	2.42	-0.31	56	6.73	3	6.51
Fe I	4250.130	2.47	-0.37	47	6.71
Fe I	4250.797	1.56	-0.69	64	6.61	10:	5.91: ^c
Fe I	4260.486	2.40	0.06	87	6.67	10:	5.70: ^c	11	5.82
Fe I	4271.774	1.49	-0.13	109	6.47	54	6.18
Fe I	4325.775	1.61	0.01	113	6.45	40	5.93
Fe I	4383.557	1.48	0.23	132	6.37	55	5.81	28	5.49
Fe I	4404.761	1.56	-0.11	102	6.41	40	6.01	22	5.76
Fe I	4415.135	1.61	-0.58	45	6.30	27	6.31
Fe II	4178.859	2.58	-2.41	92	6.46	42	6.10
Fe II	4233.169	2.58	-1.93	134	6.46	94	6.19	31	5.35
Fe II	4258.166	2.70	-3.33	34	6.79
Fe II	4273.332	2.70	-3.27	35	6.74	46	7.09
Fe II	4296.584	2.70	-2.94	43	6.52	44	6.73
Fe II	4303.177	2.70	-2.42	88	6.50	38	6.12
Fe II	4385.387	2.78	-2.50	61	6.35	38	6.25
Fe II	4416.828	2.78	-2.53	63	6.41	41	6.33
Fe II	4489.184	2.83	-2.90	54	6.70	27	6.50
Fe II	4491.408	2.85	-2.63	69	6.61	32	6.33
Fe II	4508.289	2.85	-2.14	82	6.25	49	6.07	18	5.46
Fe II	4515.343	2.84	-2.41	84	6.53	66	6.53	13	5.57
Fe II	4520.229	2.81	-2.53	66	6.45	49	6.44	19	5.85
Fe II	4522.638	2.84	-1.96	101	6.25	71	6.14
Fe II	4555.892	2.83	-2.22	86	6.36
Sr II	4077.724	0.00	0.15	152	2.03	88	1.63
Sr II	4215.539	0.00	-0.17	149	2.29	62	1.65
Ba II	4554.036	0.00	0.16	73	1.66	42	1.67

^a This line is actually a doublet, separated by 0.20 Å, with $\log gf$ -values of 0.75 and 0.57 for the two components. Spectrum synthesis used for abundance determination.

^b Discordant abundances; not used in abundance average.

^c Uncertain equivalent widths; not used in abundance average.

3. ABUNDANCE ANALYSIS

A standard analysis using model atmospheres was made with atmospheres drawn from the Kurucz (1979) grid and with gf -values mostly drawn for experimental determinations or reliable theoretical calculations. The assumption of local ther-

modynamic equilibrium (LTE) was adopted but, in particular cases, estimates or calculations of non-LTE abundances are provided. This section describes the abundance analysis.

3.1. Atmosphere Parameters

Atmosphere parameters were found using information from a variety of sources, including ionization equilibrium of Fe lines, the Cudworth & Rees (1990) M4 distance modulus, $E(B-V)$ and $(B-V)$ values, and the Strömgren photometry of Kodaira & Philip (1984).

Strömgren photometry alone cannot provide accurate temperatures for stars hotter than about 8500 K, as the $(b-y)$ color changes very slowly for large changes in T_{eff} . The temperatures are therefore very sensitive to the exact value of the adopted reddening, and to small uncertainties in the observed $(b-y)$ color. For M4 it is particularly dangerous to rely solely on $(b-y)$ as published estimates for the reddening to the cluster have a large dispersion. Cudworth & Rees (1990) found a mean reddening of $E(B-V) = 0.40 \pm 0.04$, and a reddening slope across the cluster of 83 millimagsec⁻¹. The introduction of a slope, however, did not significantly reduce the scatter in the Cudworth & Rees (1990) reddenings. It should be noted that the Cudworth & Rees (1990) mean reddening value of 0.40 is one of the highest reddening values published for M4.

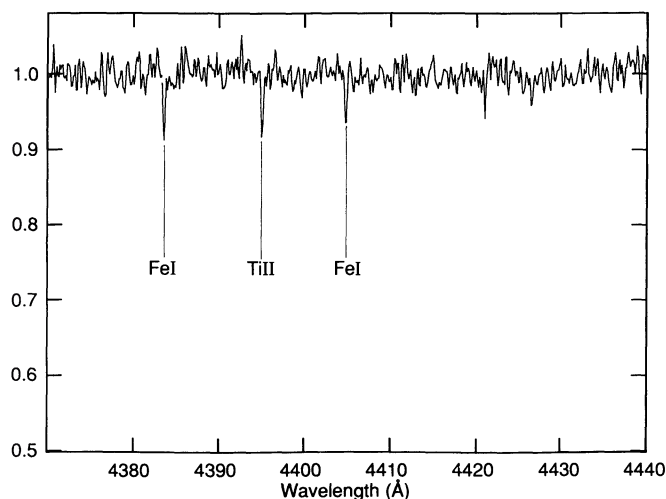


FIG. 4.—Spectrum of NGC 6397 No. 48 from 4370 to 4440 Å

In order to determine reliable temperatures, especially for the M4 stars, we used both Johnson ($B-V$) and Strömgren ($b-y$) photometry adopting a reddening which forced agreement between temperatures based on ($B-V$) and ($b-y$) colors. This method was successful because of the different temperature sensitivities of the ($B-V$) and ($b-y$) systems. The Strömgren temperature calibration used was that of Lester Gray, & Kurucz (1986), and the T_{eff} calibration of Code et al. (1976) was used for ($B-V$). With the adopted $E(B-V)$ the dereddened Strömgren c_1 index could be computed using $E(c_1) = 0.19E(b-y)$, and a $\log g$ obtained from the calibrations of Lester et al. (1986).

For star 48 in NGC 6397 the reddening values are known to ± 0.02 mag, so the difficulties encountered with the M4 stars did not occur. The reddening value of Cannon (1974) at $E(B-V) = 0.18$ was used as it is intermediate between the low value of 0.16 (Alcaino & Liller 1984) and the high value of 0.21 (Kodaira & Philip 1984).

Gravities for these cluster stars could be accurately computed using the distance modulus to the cluster, the visual magnitude, reddening, bolometric correction, and the turn-off mass of $0.8 M_{\odot}$ with equation (1):

$$\log g = \log g_{\odot} + \log M/M_{\odot} - \log L/L_{\odot} + 4 \log T/T_{\odot} . \quad (1)$$

Temperatures were also found from the spectra by deriving abundances from neutral and ionized Fe lines using the LTE model atmosphere abundance analysis. Because the model atmosphere gravities were well constrained from equation (1), the temperature could be determined by forcing Fe I and Fe II abundances to concur. However, the Fe I population can be significantly affected by non-LTE processes, causing an overionization of neutral species and depleting the Fe I population. A non-LTE analysis would yield higher Fe I abundances than the LTE analysis, and, hence, demand a more effective temperature from ionization equilibrium. A guide to the effect of non-LTE on the Fe I abundances for our AHB stars can be obtained from Gigas (1986), who performed a non-LTE abundance analysis for Fe in Vega. He found that LTE Fe I abundances are, on average, 0.32 dex below the non-LTE calculations, and that the LTE Fe II abundances are 0.02 dex greater than the non-LTE values; these corrections to LTE abundances are only weakly sensitive to the adopted surface gravity. Since our stars appear to be somewhat cooler than Vega, and in order to bring our ionization equilibrium temperatures closer to photometric temperatures, we adopt a non-LTE correction of only +0.20 dex, which we add to our LTE Fe I abundances for the purpose of temperature determination. The effect of increasing $\epsilon(\text{Fe I})$ by 0.20 dex is to decrease the ionization equilibrium temperature by about 230 K. We find that our Fe ionization temperatures, based on the corrected Fe abundances, are significantly lower than the photo-

metric temperatures for two of the three stars. In order to reduce the difference between photometric and ionization equilibrium temperatures, we adopt the highest $\log g$ values permitted from equation (1), consistent with no significant mass loss; the effect of gravity is to increase T_{eff} by 70 K for every 0.10 dex increase in $\log g$.

M4 No. 4632 provides a good example of the method employed to determine the atmosphere parameters: the Cudworth & Rees (1990) $E(B-V)$ value of 0.40 is corrected to 0.386 by the cluster reddening gradient for the position of star 4632. The observed ($B-V$) value of 0.380 gives $(B-V)_o = -0.006$, corresponding to $T_{\text{eff}} = 9560$ K on the Code et al. (1976) scale, and $(b-y)_o = -0.008$. Using the relation $E(B-V) = 1.33E(b-y)$, we find that $(b-y)_o = -0.048$, and $(c_1)_o = 1.242$, which fall outside the range of permitted values as calculated by Lester et al. (1986). The difference between the observed $(b-y)_o$ using the Cudworth & Rees (1990) $E(B-V)$, and the $(b-y)_o$ suggested from $(B-V)_o$ is 0.04 mag, which is too large to be due to observational error of the photometry; it is therefore reasonable to modify the adopted $E(B-V)$ to force agreement between ($B-V$) and ($b-y$) photometry. If $E(B-V)$ is reduced to 0.31, then $(B-V)_o = 0.07$, suggesting $T_{\text{eff}} = 9000$ K; also $(b-y)_o = +0.009$, and $(c_1)_o = 1.253$, giving $T_{\text{eff}} \approx 8950$ K and $\log g = 3.5$. The values of $\log g$ found from equation (1) are 3.5 ± 0.1 for the turn-off mass of $0.8 M_{\odot}$, and 3.2 ± 0.1 , assuming 50% mass loss.

Using a $\log g$ of 3.5, iron abundances were computed for models with T_{eff} of 9000 K and 9500 K, suggesting that the corrected Fe I and Fe II abundances would agree at $T_{\text{eff}} = 9100$ K, in satisfactory agreement with the photometric Johnson/Strömgren temperature of 9000 K. Mass loss will ensure that the mass of a HB star is less than the turn-off mass. If we attempt to account for mass loss by adopting a lower gravity of, say, $\log g = 3.20$, we find $E(B-V) \approx 0.33$, a photometric temperature of 9200 K and an ionization equilibrium temperature of 8900 K. We therefore adopt a best $E(B-V) = 0.31$, T_{eff} of 9000 ± 250 K and $\log g = 3.50 \pm 0.20$ dex.

To maintain agreement between ($B-V$), ($b-y$), and Fe ionization equilibrium $E(B-V)$ is constrained to be less than 0.33, rather than Cudworth & Rees (1990) value of 0.386. We note that our $E(B-V)$ values, found by using both ($B-V$) and ($b-y$) photometry, for the M4 stars 4408 and 4632 are 0.33 and 0.31, respectively, which compare well with the values of 0.35 and 0.33 found by Kodaira & Philip (1984).

The adopted model atmosphere parameters are listed in Table 2. The microturbulent velocity could only be found for M4 star 4408, and was adopted by forcing the iron abundance derived from Fe I lines to be independent of equivalent width, as shown in Figure 5 where abundances based on a ξ value of 3.8 km s^{-1} are plotted. Note that in Figure 5, the Fe II abundances may not be independent of equivalent width, suggesting that the microturbulent velocity is smaller for Fe II lines than the Fe I lines. For this M4 star 4632 and NGC 6397 star 48, no

TABLE 2
ADOPTED ATMOSPHERE PARAMETERS

Star	T_{eff} (K)	$\log g$ (cgs)	ξ (km s^{-1})	$[\text{Fe}/\text{H}]_{\text{model}}$	$[\text{Fe}/\text{H}]_{\text{lines}}$
M4 No. 4408	8600	3.25	3.8	-1.0	-1.05
M4 No. 4632	9000	3.50	3.8	-1.0	-1.17
NGC 6397 No. 48	9000	3.10	3.8	-2.0	-1.98

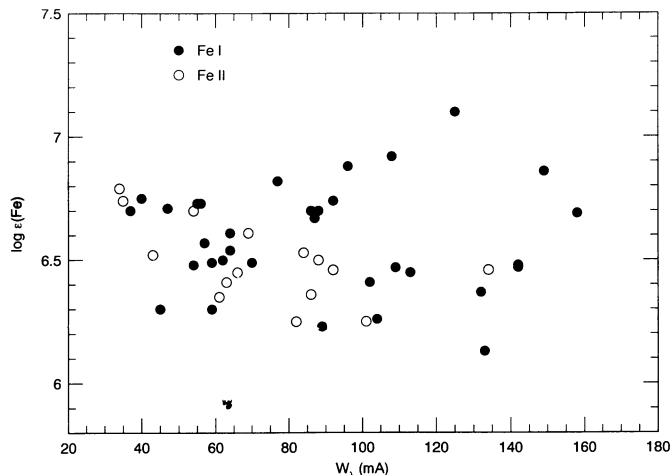


FIG. 5.—Iron abundances from Fe I (filled circles) and Fe II (open circles) lines for M4 No. 4408.

lines were strong enough to allow a ξ determination to be made, so the value of 3.8 km s^{-1} found for M4 4408 was used. This does not affect our final abundances because the lines are unsaturated and therefore, insensitive to microturbulent velocity.

Model atmospheres used in the abundance analysis came from the grid of Kurucz (1979); where necessary, the grid was interpolated to provide models of the correct temperature and gravity. Model atmospheres were selected with metallicities consistent with the derived Fe abundances. The abundance analysis employed an improved version of the spectrum synthesis program MOOG, originally written by Sneden (1974). The standard assumptions of LTE and plane-parallel atmospheres are employed by this program.

3.2. gf -Values

3.2.1. Fe Lines

For Fe II lines we adopt the log gf -values of Fuhr, Martin, & Wiese (1988) corrected by $+0.07$ dex. The correction factor is derived from the mean difference of 0.12 dex between the log gf -values of Fuhr et al. (1988) and Kurucz (1989) for 38 Fe II lines listed by Biémont et al. (1991), less a 0.05 dex correction to account for the difference between lifetime measurements made by Biémont et al. (1991) and the Kurucz (1989) log gf -values.

For most of the Fe I lines we use Oxford log gf -values (e.g., Blackwell et al. 1979a, b, 1980, 1982) listed by Fuhr et al. (1988), increased by 0.034 dex, as suggested by Bard, Kock, & Kock (1991). A number of lines came from studies by May Richter, & Wichelmann (1974), and BK (Bridges & Kornblith 1974). These two studies show no systematic trend, or offset, relative to each other, but did differ from the Oxford log gf data set, and so were normalized by Fuhr et al. (1988) onto the Oxford scale. However, Figure 4 of Fuhr et al. (1988) suggests that the BK log gf -values (for log $gf \geq -2$) are larger than the Oxford values by about 0.05 dex, and not the 0.10 dex adopted by Fuhr et al. (1988). Given that the Oxford log gf -values should be raised by 0.034 dex, the BK and May et al. (1974) log gf -values (for log $gf \geq -2$) should be decreased by only 0.016 dex, rather than the 0.04 or 0.10 dex normalizations adopted by Fuhr et al. (1988). A small subset of the Fuhr et al. Fe I log gf -values came from other sources such as Martinez-Garcia et al. (1971), Wolnik, Berthel, & Wares (1971), and

Huber & Parkinson (1972), and were normalized to the Oxford scale based on differences with the large number of lines in BK and May et al. (1974). For these lines we have accounted for the difference between the Fuhr et al. (1988), normalization of BK and the May et al. (1974) log gf -values, and our preferred normalization.

Use of the adopted gf -values gives the stellar Fe abundance. When quoting this abundance as $[\text{Fe}/\text{H}] = \log \epsilon(\text{Fe}) - \log \epsilon(\text{Fe})_{\odot}$, it is important in view of the uncertainty and confusion surrounding the solar Fe abundance to use the “appropriate” value. For the Fe II line log gf -values, the appropriate solar iron abundance is that given by Biémont et al. (1991) of 7.54 ± 0.03 . The correct solar Fe abundance for the adopted Fe I log gf -values is not immediately obvious. The Oxford group’s solar Fe I abundance at 7.673 ± 0.017 (Blackwell, Booth, & Petford 1984) is higher than the Biémont et al. (1991) value by an amount that exceeds the claimed uncertainties in the log gf -values. Holweger et al. (1991) obtain a solar abundance of 7.50 ± 0.07 from Fe I lines and gf -values based on measurements of radiative lifetimes (Bard et al. 1991). Unfortunately, our list of stellar lines and Bard et al. (1991) list of lines have no lines in common. The meteoritic Fe abundance, as established by Anders & Grevesse (1989), is 7.51 ± 0.01 .

Most of the Fe I lines used by Blackwell et al. (1984) for the solar abundance were between 60 and 90 mÅ and hence, are somewhat sensitive to the adopted microturbulent velocity. The adopted Blackwell et al. (1984) microturbulent velocity was 0.85 km s^{-1} whereas a study by Holweger et al. (1991), using a set of lines covering a large range in equivalent widths, supports a value of 1.0 km s^{-1} . For an 80 mÅ line, this difference is enough to lower the solar iron abundance by 0.10 dex below the Blackwell et al. (1984) value, which, when combined with the zero offset error of 0.034 dex in the Oxford log gf -values results in a solar Fe abundance of 7.54. For the handful of weak Fe I lines studied by Blackwell et al. (1984), the effect of microturbulence is much smaller, reducing the derived abundance by about 0.010 to 0.015 dex. However, Figure 4 of Fuhr et al. (1988) suggests a possible decrease in the Oxford log gf -values by about 0.10 dex for weak (log $gf < -2$) lines. Such a shift would not have been obvious in the BKK study, as they were restricted to strong lines. For this study we are not concerned with Fe I lines of small log gf , as our stars are quite metal-poor.

We conclude that a solar Fe abundance of 7.54 is appropriate for both Fe I and Fe II log gf -values adopted here.

3.2.2. CNO Lines

The gf -values for the C I lines are taken from Nussbaumer & Storey (1984)—see Grevesse et al. (1991) for a discussion of the C I gf -values. The gf -values for N I lines were reviewed by Grevesse et al. (1990). We adopt their recommendations and use the LS-coupling line strengths to compute values for lines not listed by them. For the O I lines, we combine LS-coupling line strengths with the multiplet gf -values calculated by Butler & Zeippen (1991).

3.2.3. Other Lines

In general, recent compilations or papers were consulted for gf -values, mostly based on laboratory experiments. For the Al I, Si I, Si II, Ca I, Sr II, and Ba II, the values come from Wiese & Martin (1980). For the few Mg I and Mg II lines, we used Jönsson et al. (1984) and Gigas (1988), respectively. The gf -values of the Si II 3856 and 3862 Å lines were taken from Wiese,

TABLE 3
C, N, AND O LINES IN M4 No. 4408

Species	λ (Å)	EP (eV)	$\log gf$	EW (mÅ)	$\epsilon(M)$
C I	9061.5	7.48	-0.35	160	7.67
C I	9062.5	7.48	-0.46	119	7.46
C I	9078.3	7.48	-0.58	119	7.58
C I	9088.5	7.48	-0.43	128	7.50
C I	9094.9	7.49	+0.15	243	7.91
C I	9111.8	7.49	-0.29	157	7.59
N I	8184.9	10.33	-0.26	51	8.12
N I	8188.0	10.33	-0.29	56	8.22
N I	8216.3	10.34	+0.11	127	8.03
N I	8242.4	10.34	-0.26	66	7.84
N I	8629.2	10.69	+0.08	105	8.11
N I	8683.4	10.33	+0.11	126	8.04
N I	8686.1	10.33	-0.29	98	8.19
N I	8703.2	10.33	-0.27	87	8.07
N I	8711.7	10.33	-0.18	79	7.91
N I	8718.8	10.34	-0.34	84	8.11
N I	9392.8	10.69	+0.35	176	8.53
O I ^a	9266.0	10.74	+0.82	142	8.02
O I ^a	9262.8	10.74	+0.67	123	7.99
O I ^a	9260.9	10.74	+0.46	81	7.87

^a Line affected by fine-structure splitting; spectrum synthesis used to compute abundance.

Smith, & Miles (1969). For Sc II, Ti II, Cr I, and Cr II, we took values from Martin et al. (1988).

3.3. The Abundances

The abundances obtained from the observed lines and a model atmosphere having the adopted parameters are listed for individual lines in Tables 1 and 3. The sensitivity of the abundances to changes of the atmospheric parameters may be gauged from Table 5. Mean abundances for each species are summarized in Table 4. A few lines were not considered in

TABLE 5
SENSITIVITY OF THE ABUNDANCES TO CHANGES OF THE MODEL ATMOSPHERES^a

Species	$\Delta T = -300$ K	$\Delta \log g = -0.25$	$\Delta \xi = -0.8$ (km s ⁻¹)
C I	-0.13	+0.03	+0.09
N I	+0.03	-0.04	+0.07
O I	+0.04	-0.05	+0.06
Mg I	+0.19	+0.07	+0.04
Al I	-0.24	+0.07	+0.16
Si I	-0.24	-0.05	+0.07
Si II	+0.09	-0.10	+0.12
Ca I	-0.27	-0.12	-0.02
Ca II	-0.31	-0.11	+0.30
Sc II	-0.17	-0.04	+0.07
Ti II	-0.14	-0.05	+0.13
Cr I	-0.28	+0.01	+0.03
Cr II	-0.08	-0.06	+0.01
Fe I	-0.26	+0.07	+0.16
Fe II	-0.10	-0.06	+0.09
Sr II	-0.27	+0.02	+0.43
Ba II	-0.29	+0.05	+0.09

^a Changes are given with respect to abundances obtained with the model $T_{\text{eff}} = 8600$ K, $\log g = 3.25$, $[A/H] = -1.0$, $\xi = 3.8$ km s⁻¹.

forming the mean abundances: e.g., the Al I 3961 Å line which is in the wing of a Balmer line.

The line-to-line scatter of the abundances is well displayed in Figures 5 and 6 for M4 No. 4408. This scatter is determined primarily by the errors in the measured equivalent widths and the adopted gf -values. The peak-to-peak range of ± 0.4 dex (Fig. 6) in the Ti abundance is independent of the equivalent width. The weaker Fe I lines ($W_{\lambda} \lesssim 80$ mÅ) show a scatter of ± 0.25 dex, but the scatter appears larger for the stronger lines. Although this increase may reflect the simple fact that a given error—fractional or absolute—in the equivalent width translates to a larger error in abundance for the stronger lines, it is

TABLE 4
AVERAGE ABUNDANCES

SPECIES	SUN $\Sigma(M)^a$	M4 No. 4408				M4 No. 4632				NGC 6397 No. 48			
		$\Sigma(M)^b$	[M/Fe]	$\sigma(M)$	N	$\Sigma(M)^b$	[M/Fe]	$\sigma(M)$	N	$\Sigma(M)^b$	[M/Fe]	$\sigma(M)$	N
C I	8.60	7.56	+0.01	0.08	5
N I	8.00	8.06	+1.11	0.12	10
O I ^c	8.93	7.96	+0.08	0.08	3
Mg I	7.58	7.23	+0.70	0.04	2
Mg II ^c	7.58	5.33	-0.27	...	1
Al I	6.48	5.67	+0.24	...	1	5.34	0.03	...	1	5.15	+0.65	...	1
Si I	7.55	6.36	-0.14	...	1
Si II	7.55	6.98	+0.48	0.22	3	7.21	+0.83	0.15	2	5.79	+0.22	0.05	2
Ca I ^d	6.34	5.76	+0.45	...	5	5.26	+0.07	0.30	3
Sc II	3.09	2.30	+0.26	0.12	5	2.04	+0.12	...	1	1.17	+0.06	...	1
Ti II	4.93	4.42	+0.54	0.21	26	4.21	+0.45	0.34	19	3.30	+0.35	0.21	9
Cr I	5.68	4.98	+0.35	...	1
Cr II	5.68	4.68	+0.05	...	1	4.49	-0.02	...	1
Fe I ^e	7.54	6.58	-0.96	0.22	33	6.12	-1.42	0.29	14	5.60	-1.94	0.20	5
Fe II ^e	7.54	6.49	-1.05	0.16	15	6.37	-1.17	0.29	13	5.56	-1.98	0.21	4
Sr II	2.93	2.16	+0.28	0.18	2	1.64	-0.12	0.02	2
Ba II	2.21	1.66	+0.50	...	1	1.67	+0.63	...	1

^a Solar system (meteoritic) abundances from Anders & Grevesse (1989) with the exception of C (Grevesse et al. 1991), N (Grevesse et al. 1990), and Fe (see text).

^b $\Sigma(M) = \log \epsilon(M)$. Fe II abundance adopted for metallicity.

^c Spectrum synthesis used to determine abundance.

^d Well-defined lines at 4226 and 4302 Å given double weight.

^e Fe abundances are relative to Sun (i.e., $[Fe/H]$) and are LTE values. The Fe II based abundance is insensitive to non-LTE effects.

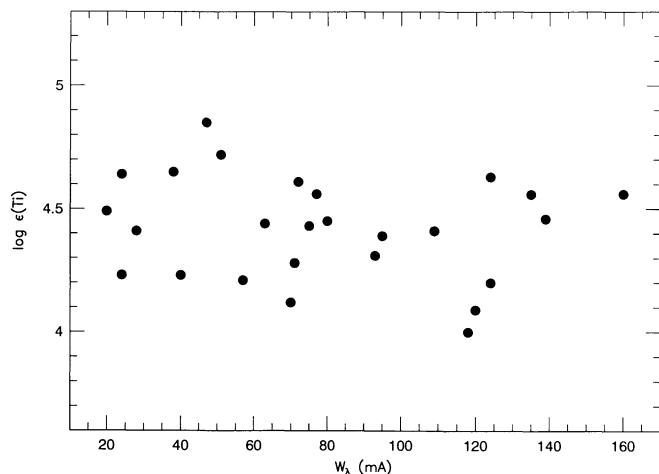


FIG. 6.—Titanium abundances from Ti II lines for M4 IRS 4408

odd that a similar effect is not seen for the Ti II lines. The Fe II lines show a small scatter (± 0.4 dex), and possibly the abundance may be lower for the strongest lines. It should be noted that the lines listed in Table 1 and used for Figures 5 and 6 are essentially all of the Fe I, Fe II, and Ti II lines in the spectrum for which accurate gf -values are available; i.e., lines were not removed from the sample because they gave a discrepant abundance. The modest scatter in Figures 5 and 6 is a testament to the spectrometer's ability to acquire high-quality spectra of faint stars by the coaddition of many spectra, each of low signal-to-noise.

An assessment of the effects of departures from LTE on the abundances may be made for Fe, Mg, and Ba from calculations done by Gigas (1986, 1988). It was noted above that the Fe abundance from Fe I lines must be increased to allow for non-LTE effects, principally the overionization of Fe neutral atoms. The non-LTE effects on the Fe II lines are predicted to be very small (less than 0.03 dex) and are ignored here. In what follows, we take the Fe abundance to be the LTE value provided by the Fe II lines. For Mg I and Mg II lines, the corrections to be applied to the LTE abundances are probably less than 0.1 dex and are ignored. For the weak Ba II 4554 Å line in Vega, Gigas predicted the non-LTE abundance should be about 0.3 dex larger than the LTE value with little sensitivity to effective temperature and surface gravity. Gigas (1988) further showed that the correction was changed only slightly when the C and Si abundances were reduced by a factor of 10 in order to reduce the ultraviolet opacity. This test is a crude simulation of conditions in the atmospheres of our more metal-poor stars. In short, the calculations of Ba in Vega indicate that our LTE Ba abundances underestimate the Ba abundance by around 0.3 dex.

4. DISCUSSION

4.1. NGC 6397

The metallicity derived here for NGC 6397 No. 48 is $[\text{Fe}/\text{H}] = -1.96$ (see Table 4) which is in agreement with published estimates from spectroscopy and photometry of the cluster's red giants. Pilachowski (1984) and Zinn (1985), who reviewed and compiled the then available data, recommended $[\text{Fe}/\text{H}] = -2.24$ and -1.91 , respectively. More recently, Caldwell & Dickens (1988) fitted synthetic spectra to 0.5 Å

resolution spectra of three red giants to obtain $[\text{Fe}/\text{H}] = -1.85 \pm 0.1$. We do not confirm KP's estimate that $[\text{Fe}/\text{H}] \approx -1.4$.

The principal reason for KP's higher metallicity would appear to be that they overestimated the equivalent widths of the lines. KP's Fe abundance is based on one uncertain measurement of a Fe II line ($\lambda 4233$) for which we measure a smaller equivalent width ($W_\lambda = 31$ mÅ versus KP's 75 mÅ). Our equivalent widths for the Al I and Si II lines are similarly smaller than KP's estimates. It should also be noted that KP's estimate of $[\text{Fe}/\text{H}]$ is based in part on the Al, Si, Ca, V, and Sr abundances and an assumption that the elemental abundance ratios with respect to iron were identical to their solar ratios. Since the α -elements Si and Ca are most probably overabundant relative to Fe, as they are in other globular clusters and in field halo stars, this assumption results in a systematic overestimate of the inferred metallicity by about 0.4 dex.

Our spectra provide measurable lines of several elements besides Fe. The lone Sc II line gives the abundance ($[\text{Sc}/\text{Fe}] = +0.06$) expected of a metal-poor field star (Lambert 1989). The several Ti II lines yield consistent estimates of the Ti abundance: $[\text{Ti}/\text{H}] = -1.63$ and $[\text{Ti}/\text{Fe}] \approx +0.3$. Such an overabundance (relative to Fe) is consistent with that found for halo field stars. Silicon is similarly overabundant: $[\text{Si}/\text{Fe}] = +0.22$. However, Mg, another α element which generally is as abundant as Si, appears underabundant: $[\text{Mg}/\text{Fe}] = -0.27$. Although this estimate is based on a single Mg II feature, it seems unlikely that the equivalent width was so underestimated that the "normal" abundance ($[\text{Mg}/\text{Fe}] \approx +0.4$) is within the margin of error—see Figures 5 and 6 for a measure of the scatter provided by a spectrum of similar quality to that obtained from NGC 6397 No. 48. Unfortunately the Mg II 4481 Å feature is too strong in the M4 stars to offer a clue to the problem. Aluminum provides a striking departure from the abundance pattern found for halo field stars: we find $[\text{Al}/\text{Fe}] \approx +0.7$, but field stars generally have $[\text{Al}/\text{Fe}] \sim 0$ at $[\text{Fe}/\text{H}] \sim -2.0$ (Lambert 1989). Although additional spectra should be obtained to confirm this Al overabundance, it seems possible that star IRS 48 is an example of the Al-rich globular stars seen among the red giants of some globular clusters and associated with the CN-strong stars in those clusters containing CN-weak and CN-strong red giants (e.g., NGC 6752—see Norris et al. 1981). NGC 6397 is so metal-poor that the CN bands are not detectable and, hence, giants cannot be classified according to CN band strength. Since the two stars in M4 have a normal Al/Fe ratio, it appears unlikely that the Al overabundance is due to an unsuspected blend. The CN-weak and CN-strong red giants in M4 do not differ in their Al abundances (Campbell & Smith 1987). Na overabundances in the CN-strong red giants are more pronounced than Al overabundances. Clearly, it would be of interest to observe Na I lines in NGC 6397 IRS 48.

4.2. M4

The metallicity of M4 as given by the Fe II lines is $[\text{Fe}/\text{H}] = -1.05$ and -1.17 for 4408 and 4632, respectively; the difference is not significant (see Table 5). These results for horizontal branch stars are in good agreement with a similar model atmosphere analysis of four red giants by Brown, Wallerstein, & Oke (1990). Their results for the individual stars were $[\text{Fe}/\text{H}] = -1.45$., -1.25 ., -1.35 ., and -1.30 where the colon is used in its traditional sense to denote an uncertain value. If half-weight is given to the uncertain values, the mean is

$[\text{Fe}/\text{H}] = -1.32$ which is based on solar gf -values. Since a solar Fe abundance of $\log \epsilon(\text{Fe}) = 7.67$ was used with a reliable empirical model to compute the solar gf -values, one would suppose that the Brown et al. (1990) cluster $[\text{Fe}/\text{H}]$ should now be raised by 0.13 dex to match the lower solar Fe abundance used by us and suggested by recent determinations of the photospheric abundance. Brown et al. (1990) compare their solar gf -values and those tabulated by Fuhr et al. (1988) and conclude that "it seems probable that our $[\text{Fe}/\text{H}]$ value should be adjusted upward by 0.1 dex because of our choice of solar gf -values". With such an adjustment their cluster metallicity is $[\text{Fe}/\text{H}] = -1.2$ and is in very good agreement with our mean of -1.1 . These metallicities agree well with most previous determinations by a variety of techniques—see the critical compilations by Pilachowski (1984) and Zinn (1985) who recommended -1.23 and -1.28 , respectively. Our and other $[\text{Fe}/\text{H}]$ determinations do not support the value of $[\text{Fe}/\text{H}] = -0.4$ obtained by KP. The discrepancy is attributable to a combination of effects: KP's equivalent widths are on average larger than ours; small differences in the gf -values; KP's atmospheres were hotter by about 300 K and of lower surface gravity by about 0.25 dex than our adopted atmospheres.

The C, N, and O abundances for 4408 given in Table 4 are LTE results. For C I, the non-LTE effects were estimated by Lemke (1991) using the model atom provided by Stürenberg & Holweger (1990): the mean abundance LTE of the lines with $W_\lambda \leq 160$ mÅ is $\log \epsilon(\text{C}) = 7.56 \pm 0.04$, and this is reduced by about 0.4 dex when the departures from LTE are considered. Then, the C abundance is $\log \epsilon(\text{C}) = 7.1$. If the apparently discrepant line at 9392 Å is excluded, the sample of N I lines give consistent abundances with a mean $\log \epsilon(\text{N}) = 8.06 \pm 0.12$. This LTE abundance may need a small revision downwards to account for non-LTE effects. However, the N I lines are much weaker than the C I lines and the LTE N abundances is independent of equivalent width in the range 50 to 130 mÅ. The 9392 Å gives a higher N abundance even when the equivalent width is measured from the lowest possible continuum level and the microturbulence is increased to the maximum extent possible: these changes reduce the abundance of 8.53 in Table 3 to 8.21. We presume this line is subject to greater than average non-LTE effects. The mean LTE O abundance is $\log \epsilon(\text{O}) = 7.96$, which is probably a slight overestimate of the correct abundance. In summary, the C, N, O abundances are (C, N, O) = (7.1, 8.1, 8.0) for 4408.

As explained in the Introduction, it is of interest to compare these CNO abundances with those of red giants. Brown et al. (1990) analyzed CH and CN lines and the [O I] 6300 Å. The [O I] line gives the O abundance almost independently of the C abundance. For the four red giants for which Brown et al. (1990) derived $[\text{Fe}/\text{H}]$, the O abundances were 7.9, 8.0, 7.85, 7.75 for a mean of $\log \epsilon(\text{O}) = 7.9$. With this O abundance, the CH lines near 4330 Å gave C abundances of $\log \epsilon(\text{C}) = 6.2, 7.0, 7.0,$ and 6.9 where the first and low value was found for a peculiar red giant with very weak CO bands in the infrared. If this star is omitted, the mean abundance is $\log \epsilon(\text{C}) = 7.0$. Finally, Brown et al. (1990) extracted the N abundance from lines of the CN Red system and the determined C and O abundances. Omitting the peculiar red giant, the three remaining giants give consistent abundances [$\log \epsilon(\text{N}) = 7.7, 8.0,$ and 7.8] and a mean $\log \epsilon(\text{N}) = 7.9$. The mean abundances obtained by Brown et al. (1990) are in excellent agreement with our results for horizontal branch: (C, N, O) = (7.0, 7.9, 7.9)

versus (7.1, 8.1, 8.0) and the agreement should not be impaired when our N and O abundances are revised downwards for non-LTE effects.

A second comparison of C abundances may be made using the data provided by Suntzeff & Smith (1991) from low resolution spectra of the CO 2.3 μm bands in 32 giants. At the lower luminosities, the giants may be assigned with fair certainty to either the RGB (i.e., evolving to the He-core flash) or the AGB (i.e., evolving from the horizontal branch.) We assign 13 and 11 stars to the RGB and AGB, respectively. The mean C abundances are $\log \epsilon(\text{C}) = 6.8$ for both samples. The star-to-star scatter in the RGB sample exceeds the likely errors of measurement. The scatter may be related to the observed spread in the strengths of CN violet band (Norris 1981; Suntzeff & Smith 1991) and, in turn, attributable to a spread in the C and N abundances. If we eliminate the few most C-poor giants from the two samples, the mean abundances are increased slightly to $\log \epsilon(\text{C}) = 7.0$ (RGB) and 6.8 (AGB). These CO-based abundances with or without the rejection of a few C-poor stars are in fine agreement with the estimate for giants from Brown et al. (1990) and our result for a HB star. Of course, the conclusion that the He-core flash does not enhance the surface C abundance requires that we assume our HB star belongs to the C-rich end of the RGB population. Additional observations of HB stars will be required to test this assumption.

The oxygen abundance $[\text{O}/\text{Fe}] = +0.1$ appears on the low end of the range expected for metal-poor stars ($[\text{O}/\text{Fe}] \simeq +0.4$, see Lambert 1989), but the uncertainty in $[\text{O}/\text{Fe}]$ is of ± 0.1 to ± 0.2 . Our LTE estimate will probably be reduced slightly when non-LTE effects are considered. Brown et al. (1990) obtain a mean $[\text{O}/\text{Fe}] = +0.3$ for their three "normal" red giants.

With the sole exception of Ba, the other elements have their expected values in the two stars. In particular, the α -elements (Mg, Si, Ca, and Ti) show an overabundance relative to Fe of about the same order as found in halo field dwarfs of the same metallicity i.e., $[\alpha/\text{Fe}] \simeq +0.4$. Titanium, the α -element best represented in our spectra, is especially close to the expectation: $[\text{Ti}/\text{Fe}] = +0.53$ and $+0.45$ in No. 4408 and No. 4632 respectively with ± 0.08 as the error of the means. The M4 red giants also show an enrichment of the α -elements (Wallerstein, Leep, & Oke 1987).

The Ba overabundance is $[\text{Ba}/\text{Fe}] \sim 0.5$ –0.6 and, as noted earlier, a correction for non-LTE effects would likely increase the abundance by an additional 0.3 dex. The resultant $[\text{Ba}/\text{Fe}] \sim 0.8$ –0.9 is at odds with measurements of metal-poor dwarfs ($[\text{Ba}/\text{Fe}] \simeq 0$) and of red giants in M4 itself ($[\text{Ba}/\text{Fe}] \simeq -0.2$, Wallerstein et al. 1987). This apparent anomaly in the HB stars warrants further study and, in particular, additional Ba II lines must be sought. Inspection of Figures 5 and 6 suggests that it is unlikely that the Ba overabundance can be attributed to an overestimate of the Ba II line's equivalent width.

5. CONCLUDING REMARKS

Our abundance analysis of horizontal branch stars on the blue side of the RR Lyrae gap shows that they have in almost every respect the composition determined previously for red giants in the same two clusters and for halo field dwarfs of the same metallicity. We do not confirm the high metallicities estimated by KP for the same three HB stars. In fact, our analysis of the C, N, and O abundances in M4 No. 4408 provides

results in remarkable agreement with the Brown et al. (1990) and Suntzeff & Smith (1991) analyses of atomic and molecular lines in M4's red giants. Although this agreement suggests that the evolution along the RGB to the HB and the early-AGB can be made without major additions to the atmosphere of the products of H and He burning, we caution that more HB stars must be studied. As noted earlier, M4 No. 4408 could be a C-poor RGB star that received an injection of C at the He-core flash and now appears as a member of the C-rich class. This scenario seems improbable, but must be tested by additional observations.

Our analysis provides one or two hints of anomalous abundances (e.g., Mg in NGC 6397 and Ba in M4). The Ba overabundance on correction for non-LTE effects is almost 1.0 dex. However, since these anomalies are based on one or two lines, we are hesitant to insist on these anomalies and to ascribe them to diffusion or to nucleosynthesis and mixing. In NGC 6752, Glaspey et al. (1988) found abundance anomalies attributable to diffusion in a HB star with $T_{\text{eff}} = 16,000$ K, but none at all in a HB star with $T_{\text{eff}} = 10,000$ K; the elements investigated were Mg, Si, and Fe in both stars, and He in the hotter star. As Glaspey et al. (1988) remark diffusion is expected to be most effective in hotter HB stars. The observa-

tions of NGC 6752 ($[\text{Fe}/\text{H}] \approx -1.5$) support the idea that our stars in M4 and NGC 6397 are unlikely candidates in which diffusion has operated.

We hope to extend our study in M4 and NGC 6397 to other HB stars on the blue and on the red side of the RR Lyrae gap. Initial location on the HB is predicted to be dependent on the envelope mass. It will be of interest to search for correlations between this mass and the chemical composition. In particular, CNO the tracers of H and He burning, should be examined. We note that the C I, N I, and O I lines are likely to be detectable in the HB stars in NGC 6397: if the C, N, and O abundances found for M4 are reduced by 1 dex, the strongest C I, N I, and O I in Table 3 have $W_{\lambda} \approx 30$ mÅ in NGC 6397 No. 48. The Al overabundance in NGC 6397 No. 48 and the Ba overabundance in the M4 stars certainly deserve further attention.

We thank M. Briley for enlightening conversations on spectroscopy of globular cluster red giants, D. Crocker for helpful discussions of the reddening of M4, and M. Lemke for undertaking non-LTE calculations. This research had been supported in part by the National Science Foundation (AST 86-14423 and 89-02835) and the Robert A. Welch Foundation of Houston, Texas.

REFERENCES

- Adelman, S. J., Fisher, W. A., & Hill, G. 1987, *Publ. Dom. Astrophys. Obs. Victoria*, 16, 203
 Alcaino, G., & Liller, W. 1984, *ApJS*, 56, 19
 Anders, E., & Grevesse, N. 1989, *Geochim. Cosmochim. Acta*, 53, 197
 Bard, A., Kock, A., & Kock, M. 1991, *A&A*, in press
 Biéumont, E., Baudoux, M., Kurucz, R. L., Ansbacher, W., & Pinnington, E. H. 1991, *A&A*, 249, 539
 Blackwell, D. E., Ibbetson, P. A., Petford, A. D., & Shallis, M. J. 1979a, *MNRAS*, 186, 633
 Blackwell, D. E., Petford, A. D., & Shallis, M. J. 1979b, *MNRAS*, 186, 657
 Blackwell, D. E., Petford, A. D., Shallis, M. J., & Simmons, G. J. 1980, *MNRAS*, 191, 445
 ———. 1982, *MNRAS*, 199, 43
 Blackwell, D. E., Booth, A. J., & Petford, A. D. 1984, *A&A*, 132, 236
 Bridges, J. M., & Kornblith, R. L. 1974, *ApJ*, 192, 793
 Brown, J. A., Wallerstein, G., & Oke, J. B. 1990, *AJ*, 100, 1561
 Butler, K., & Zeppen, C. J. 1991, *J. Phys. C*, 1, 141
 Caldwell, S. P., & Dickens, R. J. 1988, *MNRAS*, 238, 87
 Campbell, B., & Smith, G. H. 1987, *ApJ*, 323, L69
 Code, A. D., Davis, J., Bless, R. C., & Hanbury Brown, R. 1976, *ApJ*, 203, 417
 Cudworth, K. M., & Rees, R. 1990, *AJ*, 99, 1491
 Fuhr, J. R., Martin, G. A., & Wiese, W. L. 1988, *J. Phys. Chem. Ref. Data*, 17, Suppl. No. 4
 Gigas, D. 1986, *A&A*, 164, 170
 ———. 1988, *A&A*, 192, 264
 Glaspey, J. W., Michaud, G., Moffat, A. F. J., & Demers, S. 1988, *ApJ*, 329, 926
 Greenstein, J. L. 1939, *ApJ*, 90, 387
 Grevesse, N., Lambert, D. L., Sauval, A. J., van Dishoeck, E. F., Farmer, C. B., & Norton, R. H. 1990, *A&A*, 232, 225
 ———. 1991, *A&A*, 242, 488
 Heber, U., Kudritzki, R. P., Caloi, V., Castelanni, V., Danziger, J., & Gilmozzi, R. 1986, *A&A*, 162, 171
 Holweger, H., Bard, A., Kock, A., & Kock, M. 1991, *A&A*, 249, 545
 Huber, M. C. E., & Parkinson, W. H. 1972, *ApJ*, 172, 229
 Jönsson, G., Kröll, S., Persson, A., & Svanberg, S. 1984, *Phys. Rev. A*, 30, 2429
 Kodaira, K., & Philip, A. G. C. 1984, *ApJ*, 278, 201
 Kurucz, R. L. 1979, *ApJS*, 40, 1
 ———. 1989, unpublished
 Lambert, D. L. 1989, in *AIP Conf. Proc. no. 183, Cosmic Abundances of Matter*, ed. C. J. Waddington (New York: AIP), 168
 Lee, S. W. 1977, *A&AS*, 27, 367
 Lemke, M. 1991, private communication
 Lester, J. B., Gray, R. O., & Kurucz, R. L. 1986, *ApJS*, 61, 509
 Martin, G. A., Fuhr, J. R., & Wiese, W. L. 1988, *J. Phys. Chem. Ref. Data*, 17, Suppl. No. 3
 Martínez-García, M., Whaling, W., Mickey, D. L., & Lawrence, G. M. 1971, *ApJ*, 165, 213
 May, M., Richter, J., & Wichelmann, 1974, *A&AS*, 18, 405
 Michaud, G., Vauclair, G., & Vauclair, S. 1983, *ApJ*, 267, 256
 Norris, J. E. 1981, *ApJ*, 248, 177
 Norris, J. E., Cottrell, P. L., Freeman, K. C., & Da Costa, G. S. 1981, *ApJ*, 244, 205
 Nussbaumer, H., & Storey, P. J. 1984, *A&A*, 140, 383
 Peterson, R. C. 1985, *ApJ*, 289, 320
 Pilachowski, C. A. 1984, *ApJ*, 281, 614
 Sneden, C. A. 1974, Ph.D. thesis, Univ. Texas, Austin
 Stürenberg, S., & Holweger, H. 1990, *A&A*, 237, 125
 Suntzeff, N. B., & Smith, V. V. 1991, *ApJ*, 381, 160
 Wallerstein, G., Leep, E. M., & Oke, J. B. 1987, *AJ*, 93, 1137
 Wiese, W. L., & Martin, G. A. 1980, *NSRDS-NBS*, vol. 68
 Wiese, W. L., Smith, M. W., & Miles, B. M. 1969, *NSRDS-NBS*, Vol. 22
 Wolnik, S. J., Berthel, R. O., & Wares, G. W. 1971, *ApJ*, 166, L31
 Woolley, R., Alexander, J. B., Mather, L., & Epps, E. 1961, *R. Obs. Bull.*, 43
 Zinn, R. 1985, *ApJ*, 293, 424